

## Zinc incorporation in human dental calculus

Raúl A. Barrea,<sup>ab\*</sup> Carlos A. Pérez<sup>a</sup> and Aline Y. Ramos<sup>ac</sup>

<sup>a</sup>Laboratório Nacional de Luz Síncrotron - PO Box 6192 - CEP 13084-971, Campinas, SP, Brazil, <sup>b</sup>Facultad de Matemática, Astronomía y Física - Universidad Nacional de Córdoba, Ciudad Universitaria - 5010 -Córdoba, Argentine, <sup>c</sup>LMPC, UMR7590, France  
Email: raul@lnls.br

We present here the first study of the local environment of zinc ions in biological calcium phosphates. It was suggested from *in vitro* studies that zinc inhibits the formation of hydroxyapatite and promotes the formation of more soluble phases, like tricalcium phosphate. Several mechanisms of zinc – calcium phosphate interaction were proposed, yielding either to the adsorption or to the incorporation of zinc ions into the phosphate structure. The results obtained here show that, under *in vivo* conditions, the zinc atoms are fully incorporated into the crystalline structure of the calcium phosphates.

**Keywords:** zinc, calcium phosphates, human dental calculus

### 1. Introduction

A calcification process of the bacterial deposits in the tooth produces Human Dental Calculus (HDC). The dental calculus is usually described as mineralised plaque covered in the external surface by strongly adhered and nonmineralised plaque (Mandel, 1987).

Mature calculus is compounded of an inorganic or mineral phase and an organic one. The mineral phase has an inorganic content similar to the bone, the dentine and the cementum. It consists mainly of a mixture of calcium phosphates including: brushite or dicalcium dihydrate phosphate ( $\text{CaHPO}_4 \cdot 2\text{H}_2\text{O}$ ); octacalcium phosphate ( $\text{Ca}_8\text{H}_2(\text{PO}_4)_6 \cdot 5\text{H}_2\text{O}$ ); magnesium whitlockite or tricalcium phosphate ( $(\text{Ca},\text{Mg})_3(\text{PO}_4)_2$ ) and carbonated hydroxyapatite ( $(\text{Ca},\text{X})_{10}(\text{PO}_4)_6(\text{HPO}_4, \text{CO}_3)_6$ ).

Besides calcium and phosphorus, HDC contain carbonates, sodium, magnesium, potassium and some residual elements such as fluorine, zinc and strontium (Knuuttila *et al.* 1979; Grøn & Campen, 1967).

It was found that zinc acts as a nucleator in the formation of the whitlockite phase *in vitro* (Knuuttila *et al.*, 1980). Zn also plays a role of inhibitor of hydroxyapatite crystallization producing  $\beta$ -tricalcium phosphate, whitlockite (Bigi *et al.*, 1997). The lattice parameters reported by Bigi *et al.* (1997) showed a contraction of the unit cell relative to pure  $\beta$ -TCP, suggesting a partial substitution of calcium by zinc ions in the structure. Several studies *in vitro* about the zinc incorporation in HA and  $\beta$ -TCP have been done by using XRD (Ingram *et al.*, 1992; Davey *et al.*, 1997; Bigi *et al.*, 1997).

The mechanisms of adsorption or incorporation of zinc ions in the lattice were proposed. If zinc is added after the achievement of calcium phosphate phases formation it only could bind on the surface. It was found that low concentrations of zinc incorporated into the synthesis of calcium phosphates promotes the

formation of amorphous calcium phosphates, ACP, under conditions where dicalcium dihydrate phosphate and octacalcium phosphate are formed (LeGeros *et al.*, 1999).

The aim of the present work is to provide information about the local environment of zinc atoms in biological samples formed under *in vivo* conditions. We carried out the present study on sub-gingival human dental calculus using the EXAFS technique.

### 2. Materials and methods

The samples consisted of two human dental calculi extracted from patients from Córdoba City, province of Córdoba, Argentine. The samples were washed in distilled water and dried at room temperature. Acrylic resin was used as mechanical support. The samples were oriented and polished so as to obtain a surface perpendicular to the oral surface of the calculus. The samples present irregular shapes with reduced areas between 2 to 6 mm<sup>2</sup>. Synthetic stoichiometric (Ca/P= 1.69) hydroxyapatite (HAP) doped with zinc was also measured. The synthetic HAP was prepared by putting 0.1 g of HAP in contact with a solution of  $\text{Zn}(\text{NO}_3)_2 \cdot 6\text{H}_2\text{O}$  with a zinc concentration of 200 ppm, under stirring during 24 hours. ZnO was used as experimental standard.

The EXAFS measurements, at the Zn K-edge, were performed at the FRX beam line at the LNLS (Pérez *et al.*, 1999), running at 1.37 GeV and 120 mA. The monochromator is a double crystal channel-cut type of Si(111). The system was calibrated at the maximum of the first derivative of Zn K edge ( $E_0 = 9659$  eV) using a metal foil as reference. Because of the low zinc concentration, the measurements were performed in fluorescence detection mode using a Si(Li) solid state detector. The signal from the detector was filtered with a single channel analyser (SCA). The SCA was calibrated at the  $\text{ZnK}\alpha$  characteristic radiation to discriminate the scattered radiation. A standard geometry of 45° incidence and take off of the radiation was used. The detector was positioned at 90° of the direction of incidence in order to reduce the scattering radiation contribution. The sub-gingival part of the calculus was selected because it has higher zinc concentration levels than the supra-gingival part. A finely collimated X-ray beam excited the selected area. Special care was taken to avoid the excitation of the supra-gingival part of the samples. The low counting rate obtained for the calculus samples, around 100 counts/sec, required multiple scans so as to obtain acceptable counting statistics. Corrections for detector nonlinearity were not necessary because of the low counting rates. Self-absorption effects were not considered because of the dilution of zinc in the sample. The synthetic HAP was measured in fluorescence detection mode using a NaI(Tl) scintillator detector of 32 mm diameter and beryllium window of 0.2 mm, using the same geometry described above with the Si(Li) detector. The ZnO standard was measured in transmission mode using two ionisation chambers filled with air at 1 atm.

The data were analysed using the WinXAS code (Ressler, 1997). A first order polynomial fitting was used to remove the pre-edge background and a fifth order polynomial was used to remove the above edge background. The raw EXAFS data were weighted by  $k^3$ , truncated at  $k=2.4$  and  $k=8.7$  Å<sup>-1</sup>. A Fourier transform was calculated and a Bessel 4 filter window was used. The first shell peak was isolated and back-transformed into  $k$ -dependent data. The best-fit distances, co-ordination numbers and Debye–Waller factors were obtained from first shell fitting of the Fourier-filtered data using experimental phase and amplitude functions obtained from the ZnO standard. We obtained another set of co-ordination numbers by using the bond valence sum method (Brown and Altermatt, 1985). These co-ordination numbers were compared with the values obtained by the EXAFS analysis.

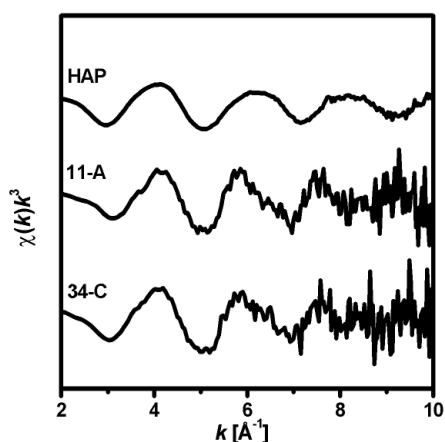


**Figure 1**  
EXAFS oscillations  $k^3$  (weighted) of the three measured samples.

### 3. Results and discussion

The EXAFS signals for the three samples are shown in figure (1). The Fourier transform of the  $\chi(k)k^3$  gives the pseudo radial distribution function (figure (2)). The first peaks of the 11-A and 34-C biological samples, attributed to Zn-O, are centred at a greater R value than the synthetic HAP's peak. The first shell contribution was isolated and fitted by using Zn-O experimental phase and amplitude functions obtained from the ZnO standard (4 oxygen atoms at a distance  $R_{\text{Zn-O}}=1.98$  Å). The raw EXAFS data, the first shell contribution and the first shell fit of sample 11-A are shown in Fig. 3.

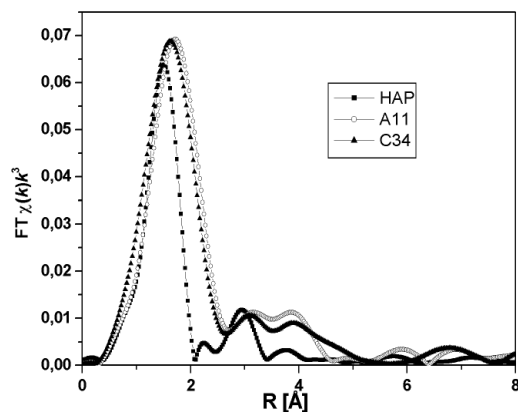


**Figure 2**  
Fourier transform of the  $k^3$  weighted EXAFS signal for the three samples.

The results of the fitting procedure are given in table 1. In the synthetic HAP the co-ordination number as well as the Zn-O distance indicate a tetrahedral environment of zinc atoms, like the ZnO standard. The Zn-O distances and co-ordination numbers found for the biological samples indicate a larger number of co-ordination ligands than the synthetic sample. The co-ordination numbers found by EXAFS analysis are in good agreement with the values obtained by the Bond Valence Sum Method (BVSM), except in the case of sample 11-A where the EXAFS co-ordination number is approximately 4. The values obtained with the BVSM are consistent with the bond length reported here.

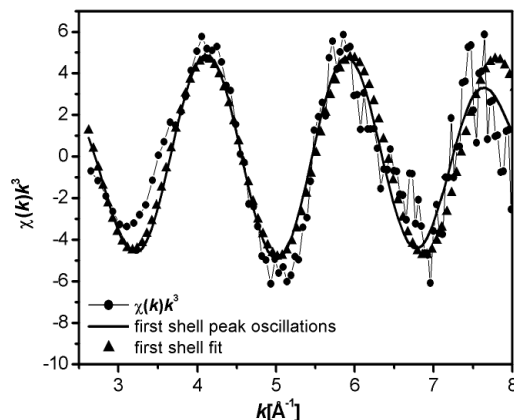


**Figure 3**  
Raw EXAFS, first shell and curve fitting of the first shell oscillations of sample 11-A.

As already mentioned, the dental calculus is a mixture of several calcium phosphates phases, mainly whitlockite and hydroxyapatite. As previously suggested (Bigi *et al.*, 1997) the six fold coordinated site M(V) of the whitlockite structure, presents the most favourable environment for zinc ions. The two cation sites in the hydroxyapatite structure, which are six fold coordinated also, indicate that zinc is localised in a cation site into the calcium phosphate lattice in both samples. The relatively short distance found for the Zn-O (2.06 Å) compared to the Ca-O (2.25 Å) distance (Dickens *et al.*, 1974; Sugiyama *et al.*, 1996) can be explained by considering the small ionic radius of the zinc ion (0.74 Å) than the calcium ion (0.99 Å) that produces a contraction of the cationic site. The present results suggest an active participation of the zinc atoms in the biological synthesis of these calcium phosphates.

Sample	HAP	11-A	34-C
Distance (Å)	1.98±0.02	2.08±0.03	2.06±0.03
DW Factor [Å²]	0.003±0.002	0.003±0.002	0.003±0.002
Eo shift [eV]	-3.9±0.6	3.6±1.0	2.2±0.8
EXAFS Coord. Number	4.0±0.2	4.2±0.8	5.1±0.8
BVSM Coord. Number	4.2±0.4	5.5±0.9	5.2±0.9

**Table 1**  
Near neighbour Zn-O distance, co-ordination number, Debye-Waller factor and energy shift obtained by fitting the first co-ordination shell around zinc in both subgingival HDC and synthetic HAP. The co-ordination numbers obtained by the Bond Valence Sum Method (BVSM) are also indicated.

Because of the similar environment of the whitlockite and hydroxyapatite cation sites and the relatively poor signal to noise of the EXAFS data, it was not possible to identify in which structure the zinc atoms are really located. New measurements are being performed in order to elucidate this point.

### 4. Conclusions

The first direct determination of the local environment of zinc in biological calcium phosphates was reported here. The environment of zinc found by EXAFS analysis is compatible with a Zn to Ca substitution into the lattice. This result suggests that zinc ions have an active participation in the synthesis of the calcium phosphates under *in vivo* conditions.

Research partially supported by LNLS – National Synchrotron Light Laboratory, Brazil, FAPESP and CNPq. One of the authors (R. A. B.) has a CLAF/CNPq post-doctoral fellowship. We are grateful to Miriam Grenón (Facultad de Odontología – Universidad Nacional de Córdoba, Argentina) for the dental calculi provided and Dr. Alexandre Rossi (CBPF - Brasil) for providing the synthetic hydroxyapatite.

### References

- Bigi, A., Foresti, E., Gandolfi, M., Gazzano, M. & Roveri N., (1997), *J. Inorg. Biochem.* 66, 259-265.
- Brown I. D. & Altermatt D., (1985), *Acta Cryst.* B41, 244-247.
- Davey H. P., Embery G. & Cummins D., (1997), *Caries Res.* 31, 434-440.
- Dickens B., Schroeder L. W. & Brown W. E., (1974), *Journal of Solid State Chemistry* 10, 232-248.
- Grøn P. & van Campen G. J., (1967), *Helv. Odont. Acta*, 71-74.
- Ingram G. S., Horay C. P. & Stead W. J., (1992), *Caries Res.* 26, 248-253.
- Knuuttila M., Lappalainen R. & Kontturi-Narhi V., (1979), *Scand. J. Dent. Res.* 87:192-196.
- Knuuttila M., Lappalainen R. & Kontturi-Narhi V., (1980), *Scand. J. Dent. Res.* 88:513-516.
- LeGeros R. Z., Bleiwas C. B., Retino M. Rohanizadeh R. & LeGeros J. P., (1999), *Am. J. Dent.* 12, 65-70.
- Mandel I.D., (1987), *Calculus formation and prevention: an overview. Compend. Contin. Educ. Dent.; Suppl.8: S235-241.*
- Pérez C. A., Radtke M., Sánchez H. J., Tolentino H., Neuenschwander R. T., Barg W., Rubio M., Bueno M. I. S., Raimundo I. M. & Rohwedder J. J.R., (1999), *X-Ray Spectrom.* 28, 320-326.
- Ressler T., (1997), *J. Physique C2-269-C2-270.*
- Sugiyama S., Minami T., Moriga T., Hayashi H., Koto K., Tripathy N. K., Patel P. N. & Panda A., (1989), *J. Solid State Chem.* 80, 1.